Journal of Autoimmunity 33 (2009) 99–108

Contents lists available at ScienceDirect

Journal of Autoimmunity

journal homepage: www.elsevier.com/locate/jautimm

Gene expression and chromosomal location for susceptibility to Sjögren's syndrome

Paola Pérez [a,1], Juan-Manuel Anaya [b,1], Sergio Aguilera [c], Ulises Urzúa [a], David Munroe [d], Claudio Molina [e], Marcela A. Hermoso [a], James Michael Cherry [d], Cecilia Alliende [a], Nancy Olea [a], Edward Ruiz-Narváez [f], María-Julieta González [a,*]

[a] University of Chile, Santiago, Chile
[b] Center for Autoimmune Diseases Research (CREA), Corporación para Investigaciones Biológicas, Universidad del Rosario, Medellin, Colombia
[c] INDISA Clinic-Andrés Bello University, Santiago, Chile
[d] National Cancer Institute, Bethesda, MD, USA
[e] Mayor University, Santiago, Chile
[f] Harvard School of Public Health, Boston, MA, USA

ARTICLE INFO

Article history:
Received 2 April 2009
Received in revised form
11 May 2009
Accepted 19 May 2009

Keywords:
Sjögren's syndrome
cDNA microarray
Epithelial cells
Apoptosis
Interferon
Genome-wide association study

ABSTRACT

Primary Sjögren's syndrome (SS) is a chronic inflammatory autoimmune disease affecting mainly the exocrine glands. Its physio-pathology is poorly understood and most of the knowledge has been related to the inflammatory component. The aim of this work was to evaluate gene expression profiling in fractions enriched in epithelial cells from labial salivary glands (LSGs) of patients with primary SS and identify chromosomal regions harboring susceptibility genes expressed in epithelial cells. A combined approach of gene expression and genome-wide association study was used. Enriched epithelial cell fractions were obtained from LSGs of patients and controls. Amplified total RNA was labeled and hybridized to 10K cDNA microarrays. Results were normalized and subjected to statistical and functional analysis. A genome-wide microsatellite screen at 10 cM resolution (393 markers) was performed. In salivary gland-epithelial cells from patients 528 genes were expressed differentially in comparison to controls. Pathways not previously linked to disease were found to be altered. Twenty-eight and 15 genes associated with apoptosis were up-regulated and down regulated, respectively. Interferon-related genes, most of which participated in interferon signaling, were also found to be up-regulated. From the genome-wide screen, 6 markers showed evidence of highly significant association with the disease. Of these, five loci harbor genes differentially expressed in patients LSG-epithelial cells. Our results show that in enriched gland-epithelial cells of pSS, both pro-apoptotic/anti-apoptotic and interferon signaling inhibition/stimulation balances may occur. Genes found over-expressed in epithelial cells are candidates for disease susceptibility.

1. Introduction

Sjögren's syndrome (SS) is a chronic autoimmune disease characterized by lymphocyte infiltration of the exocrine glands, accompanied by autoantibody production [1]. A key event in the initial process leading to SS seems to be increased epithelial cell apoptosis that progresses to subsequent salivary gland lymphocytic infiltration and autoantibody production [2,3]. High levels of matrix metalloproteinases (MMPs), mostly secreted by acinar and ductal cells but not related to the quantity and the proximity of mononuclear cells, have been demonstrated in labial salivary glands (LSG) from SS patients [4–6]. Based on these findings three phases for the development of SS are proposed: first, a preexisting condition characterized by genetic susceptibility factors. Second, a lymphocyte-independent phase which occurs as a consequence of antigens released by necrotic, apoptotic cells or viral trigger, activate innate immune response with cytokine production. Third, a tissue-specific immunological attack by activated T-cells, B-cells and their products against corresponding self-antigens leads to autoimmune exocrinopathy [1–3].

The powerful impact of genetic predisposition on susceptibility is usually based on disease concordance rates in monozygotic

* Corresponding author at: Institute of Biomedical Sciences, Faculty of Medicine, University of Chile, Casilla 70061, Santiago 7, Chile.Tel.: +56 2 9786017; fax: +56 2 737 3158.
E-mail address: jgonzale@med.uchile.cl (M.-J. González).
[1] These authors contributed equally to this work.

0896-8411/$ – see front matter © 2009 Elsevier Ltd. All rights reserved.
doi:10.1016/j.jaut.2009.05.001

twins. Although genetic studies in primary SS twins have not been performed the observed aggregation of autoimmune diseases in families of patients with primary SS supports a genetic component in SS etiology [7]. The efforts to unravel the genetic component of SS have relied on association studies for disease gene identification. However, robust analyses of candidate gene variants have not been undertaken and only one linkage study has been reported [8]. In the absence of chromosomal regions identified by linkage studies, research has focused on candidate gene approaches (by biological plausibility) rather than on positional approaches. To date, there is not any specific gene for primary SS, and all of the polymorphisms associated with primary SS have been also associated with other autoimmune diseases [9].

DNA microarray technology allows gene expression information on a wide-genome basis to be obtained. A few reports have described transcriptional profiles of whole LSG from SS patients [10–12]. A neglected aspect of these studies is that the amount of mononuclear infiltrate in LSG varies between SS patients [13]. Therefore, these gene expression profiles actually represent variable combinations of different cell types. To overcome the interference of infiltrated cells on epithelial cell gene expression, we developed a method to obtain fractions enriched in epithelial cells from LSGs and to determine their gene expression profiles using DNA microarrays. Through a genome-wide association study (GWAS) we next sought to identify chromosomal regions of SS susceptibility harboring expressed genes in LSG of SS patients.

2. Methods

2.1. Patients

All participating subjects were informed about the aims and procedures of the present study and then signed a written consent approved by the Ethics Committee of the School of Medicine, University of Chile and the "Corporación para Investigaciones Biológicas" (CIB), in Medellín, Colombia. All the patients met the American-European diagnosis criteria for primary SS [14].

For the microarray study, patients ($n = 9$) were classified according to the focus score (FS) [13]: FS 1–2 ($n = 2$, age range 43–60 years old, mean 51); FS 3–4 ($n = 3$, age range 35–66 years old, mean 48); FS higher than 4 ($n = 4$, age range 35–64 years old, mean 54). Control subjects ($n = 6$, age range 23–43 years old, mean 35) were selected from individuals not meeting the SS classification criteria. All control subjects were negative for rheumatoid factor, antinuclear antibodies and anti-Ro and anti-La antibodies. Mild and nonspecific inflammation (Chisholm and Mason grade 1) was observed in lip biopsies from the control group.

For the GWAS, 85 women with primary SS and 178 ethnic-, gender-, age- and socioeconomic-matched controls, belonging to a homogeneous population [15,16], were included (Supplementary data STable 1).

2.2. Preparation of a cell fraction enriched in epithelial cells from labial salivary glands

LSGs were digested in 10 mL of DMEM pH 7.4 (Gibco BRL, Carlsbad, CA) containing 1 mg/mL of collagenase IV (Sigma–Aldrich, St. Louis, MO) for 30 min at 37 °C and shaken at 120 cycles/minute. Then, the suspension was incubated in fresh collagenase-containing medium for 45 min. Mechanical disaggregation was done by passing the cell suspension through a series of three Pasteur pipettes of decreasing tip diameters (2.0, 1.0 and 0.5 mm). After the third pipetting round, the suspension was centrifuged for 5 min at 1.9 × g at 4 °C, the supernatant discarded and the pellet re-suspended in a collagenase-free medium. Epithelial cell suspensions were further washed with Hanks' balanced salt solution (Gibco BRL, Carlsbad, CA, USA) and then centrifuged for 5 min at 1.9 × g at 4 °C. Washes were repeated from 3 to 12 times according to the extent of infiltration observed in each LSG biopsy until no lymphocytes were observed in the supernatant or pellet. This was verified by direct microscopic observation of an aliquot of supernatant or pellet of epithelial cells. The short-time, low-speed centrifugation and extensive washes resulted in a pellet containing mostly epithelial (acini and ducts) material. The final pellet was split to extract RNA for gene expression assays (see Section 2.3) and for morphological analysis as follows: aliquots were taken at each isolation step and fixed at 4 °C for 18 h in a glutaraldehyde 2.5%-sodium caccodylate 0.1 M pH 7.4 buffer. Then, they were rinsed in a caccodylate buffer and post-fixed in a 1% osmium tetroxide-0.1 M caccodylate buffer pH 7.4 for 1 h. Dehydration in graded series of ethanol was done before infiltration in an epoxy resin. Acinar fraction sections (1 μm) were obtained by means of a Porter-Blum ultramicrotome (Sorvall MT-2, Thermo Electron Corporation, Asheville, NC, USA) and stained with toluidine blue in 1% sodium borate. In addition, the quality of the resultant cellular fractions was verified by reverse transcriptase-polymerase chain reaction (RT-PCR) [5] of marker genes such as: MS4A1, CD3G, ACTA2, and KRT18 as markers for B-lymphocytes, T-lymphocytes, myoepithelial cells and acinar-ductal cells, respectively. Primers and reaction conditions of each gene are described in Supplementary data STable 2.

2.3. RNA isolation, amplification and fluorescent cDNA labeling

Total RNA was procured with the RNeasy Mini Kit (Qiagen, Valencia, CA, USA). Quality was verified with the Agilent 2100 Bioanalyzer (Agilent Technologies, Palo Alto, CA, USA). RNAs were amplified with the RiboAmp amplification kit (Arcturus, Sunnyvale, CA, USA) following the supplier's protocol. 2 μg of amplified RNA were labeled by reverse transcription in a 45 μL reaction containing 1× first strand buffer, 2 μg random primers, 2 μg oligo-dT, 0.5 mM of dATP, dGTP and dTCP, 0.2 mM dTTP, 0.08 mM of either Cy3 or Cy5 of dUTP, 0.01 mM dithiothreitol, and 500 U of SuperScript II enzyme (Invitrogen, Carlsbad, CA, USA). After incubation at 42 °C for 1 h, the reaction was halted with EDTA. Residual RNA was hydrolyzed with NaOH at 65 °C for 20 min. NaOH excess was neutralized by addition of Tris–HCl 1 M, pH 7.5 buffer. The labeled cDNA was purified by ethanol precipitation in the presence of 20 μg of glycogen. Absorbance readings at 260, 550 and 650 nm were measured to estimate labeling efficiency.

2.4. Microarray manufacture and hybridization

Microarrays were printed on poly-lysine coated slides using a MicroGrid II arrayer (Biorobotics, Boston, MA, USA) at the Laboratory of Molecular Technology, SAIC-NCI Frederick. Spotted DNAs consisted of 9961 distinct PCR-amplified human cDNAs prepared from the IMAGE-EST clone collection. The printed pattern and the complete clone list are available at the NCI's Microarray Database ("mAdb") (http://nciarray.nci.nih.gov/cgi-bin/Hsatcincyteform.cgi). Labeled test and reference (a pool of control individuals) cDNAs were combined at approximately Cy3/Cy5 equimolar quantities and co-hybridized in 38 μl solution containing final concentrations of 1 μg/μl human Cot-1 DNA, 1 μg/μl poly dA, 0.1% SDS and 3.5× SSC. This mixture was denatured at 99 °C for 3 min, cooled at room temperature, and deposited onto the array surface. Microarrays were placed in hybridization chambers and incubated at 65 °C for 14–18 h in a water bath. Washes in 2× SSC-0.1% SDS, 1× SSC, 0.2× SSC and 0.05× SSC were performed, 1 min each. Microarrays were dried and scanned at 10 μm resolution in a GenePix 4000B scanner

(Axon Instruments, Union City, CA). Voltage was adjusted to obtain maximal signal intensities with minimal (<0.1%) probe saturation. Pseudocolor microarray images were saved in tiff format.

2.5. Validation of microarray results

Quantitative PCR (Q-PCR) assays of selected genes, as well as immunohistochemical localization and expression of the MSN protein were performed as microarray data validation. Briefly, specific primer pairs for the 3′-mRNA ends of test (HLA-DPA1, MMP-9, MSN and VIM) and reference (GAPDH) mRNAs were obtained with the Assay-by-design software (Applied Biosystems, Foster City, CA, USA). The cDNAs were prepared by reverse transcribing 1 μg of amplified RNA with the Superscript II enzyme (Invitrogen, San Diego, CA, USA). Q-PCR assays were conducted in 384-well microtiter plates in 10 μL final volumes. PCR cycles in the Applied Biosystems ABI-7900 SDS thermocycler were 50 °C for 2 min, 95 °C for 10 min and 40 cycles of 95 °C for 10 s and 60 °C for 1 min. Quantification was based on C_T values, which represent the PCR cycle at which an increase in reporter fluorescence above baseline signal can be detected. Normalization employed the GAPDH gene value as reference transcript assayed under identical conditions respective to the gene of interest. Numerical conversion of C_T values to microarray ratios was based in reverse $\Delta\Delta C_{T\text{-}Sample}$ values, were $\Delta\Delta C_{T\text{-}Sample} = \Delta\Delta C_{T\text{-}Sample} - \Delta C_{T\text{-}Reference}$. For MSN protein validation, samples were fixed in 1% paraformaldehyde for 6 h and then embedded in paraffin. Sections were assayed for epitope recovery by heating at 95 °C for 20 min in 10 mM citrate buffer (pH 6.0). Endogenous peroxidase activity was quenched with 0.3% H_2O_2 in methanol, and nonspecific binding was blocked with 0.25% casein during 30 min. Sections were incubated with a monoclonal antibody against human MSN (BD Biosciences, San Jose, CA) followed by incubation with a rabbit anti-mouse Alexa fluor 488 antibody (Molecular Probes, Invitrogen, CA). For nuclear counterstaining, the sections were incubated in 1 μg/mL propidium iodide, 1 μg/mL RNAse A in phosphate buffer pH 7.4 for 1 min. The pre-immune controls were also performed.

2.6. Microarray data extraction and analysis

All microarray data presented here is in the two-color comparative format, i.e., it corresponds to the $\log_2$-expression ratio of the fluorescent signal in the test sample over the fluorescent signal in the reference sample for every single gene spotted on the array. Microarray tiff images were extracted as GenePix result (gpr) files using the GenePix Pro III software (Molecular Devices CA). Gpr files and jpeg array images were deposited at mAdb. Data were subsequently subjected to print-tip (local) Loess normalization and scale correction with the DNMAD tool. (http://dnmad.bioinfo.cnio.es) [17]. Genes which were present in less than 85% of the arrays were excluded from the analysis. Missing values were imputed using KNN-impute (weighted K-nearest neighbors) at GEPAS (http://gepas.bioinfo.cnio.es/cgi-bin/preprocess) [18]. At this point, the dataset size was reduced to 4866 clones. Patient data was compared with control data using a limma *t*-test with adjustment for multiple testing performed with the tool Pomelo II (available at: http://pomelo2.bioinfo.cnio.es/). A total of 627 cDNA clones were detected as differentially expressed using an adjusted $p < 0.05$ as cut-off. After excluding repeats, transcribed loci and unknowns, the 627 list was reduced to 528 known genes that were the subject of functional analysis. Correlation of transcriptional profiles with lymphocytic infiltrate (i.e., FS) was done with the multiple testing tools Pomelo (http://pomelo.bioinfo.cnio.es/) with false discovery rate (FDR) control.

2.7. DNA preparation and genotyping

Genomic DNA was extracted from 10 mL of an EDTA-anticoagulated blood sample using the classical salting out protocol. Three hundred ninety three polymorphic Marshfield microsatellite markers with an average spacing of ~10 cM from Marshfield Screening Set 16 were genotyped by the Marshfield Center for Medical Genetics (http://research.marshfieldclinic.org/genetics/).

2.8. Genetic analysis

Allele frequencies in each microsatellite marker locus in the SS cases and matched controls were estimated by the gene-counting method. We assessed whether there was any hidden population stratification by using the model-based clustering method under an admixture model as implemented in the Structure software version 2.2 [19]. Briefly, the admixture model assumes that different *K* populations contribute to the genomic composition of our sample [19]. Each individual in the sample had different genomic proportions of each of the *K* populations. We ran the admixture model under three different number of populations ($K = 1$, 2, and 3) using 10,000 Markov Chain Monte Carlo simulations for each *K*. The structured population association test (STRAT) [20], using 10,000 Markov Chain Monte Carlo simulations for each marker, was applied to test for differences in the microsatellite allele frequencies between SS cases and controls. We used a $-\log(p\text{-value}) = 2$, equivalent to a p-value = 0.01, to determine significance.

3. Results

3.1. Analysis of fractions enriched in acinar and ductal epithelial cells

In order to examine the molecular events occurring in the LSG-epithelial cells of SS patients, we obtained a cellular fraction enriched in acinar and ductal cells. The quality of the fraction was analyzed morphologically. Fig. 1 shows panoramic views of sections of enriched epithelial fractions from one control (A) and two patients (C and D). The control sample displayed many acini with narrow lumen, and acinar cells with typical polarized morphology showing the nucleus located at the basal region and the secretory granules at the apical region. Details of a seromucous acinus are shown at higher magnification in Fig. 1B. In SS patients, acini clusters of variable-size and characteristic luminal dilation were observed in association with intercalated ducts; the inset shows details of a seromucous acinus (Fig. 1C). Fig. 1D shows a striated duct among several acini (see details of striated duct in the corresponding inset). Only in one from 9 SS patients a discrete cluster of inflammatory cells was found. To confirm our morphological observations markers for each cell type were monitored by RT-PCR (see Methods) which are shown in Fig. 1E (control) and 1F (SS patient). Lymphocytic cell markers (MS4A1 and CD3G) were undetectable in the enriched epithelial cell fraction (lanes E) of control samples (Fig. 1E), whereas in an SS patient, the correspondent bands (lanes E) were weaker than in the whole salivary gland (lanes G, Fig. 1F). On the contrary, epithelial markers (KRT18 and ACTA2) showed higher levels indicating epithelial cell enrichment in both groups.

3.2. Genome-wide transcriptional profile of fractions enriched in LSG-epithelial cells from SS patients

For all hybridizations, a pool of total RNA from control individuals was used as the reference, so the differentially expressed genes in SS patient samples were obtained directly. Repeated dye-swap

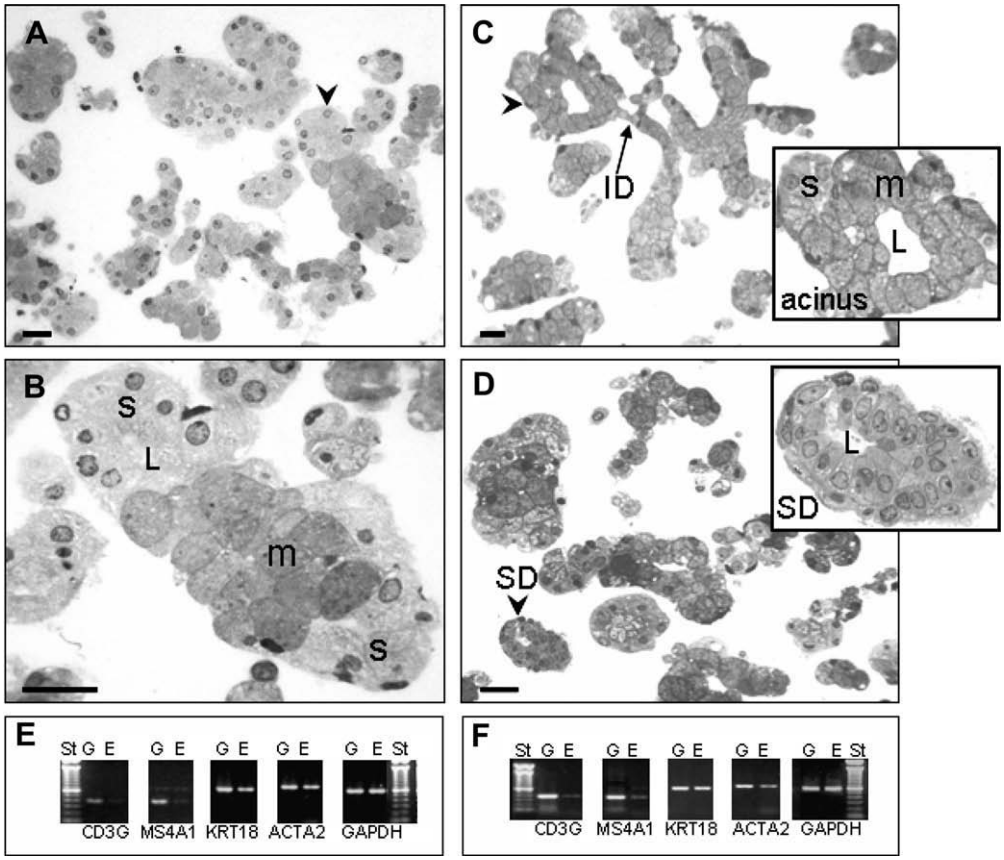

Fig. 1. Morphological and molecular analysis of enriched LSG-epithelial cell fractions. Images A–D show LSG sections stained with toluidine blue of one control subject (A, B) and two SS patients (C, D). From each preparation, randomly chosen fields are shown. Arrowhead in A indicates a seromucous acinus shown in B. Arrowheads in C and D indicate the corresponding insets. s: serous acinar region, m: mucous acinar region, L: acinar lumen, ID: intercalated duct and SD: striated duct. Bars: 21 μm. Panels E and F show RT-PCR amplification products of cell-type marker genes (CD3G, MS4A1, KRT18, and ACTA2) and the endogenous control gene (GAPDH) from whole LSG (lanes G) and enriched LSG-epithelial cell fractions (lanes E) obtained from representative controls (panel E) and SS patients (panel F). St: 100 bp ladder.

(i.e., 4 replicas for each sample) was made, resulted in 52 microarray data files which were deposited in mAdb. The mean percentage of "found" spots was 87 ± 13% and the mean signal-to-background ratios were 5.93 and 7.49 in the Cy3 and Cy5 channels respectively. Prior to statistical analysis, data were normalized using Loess analysis [17]. Normalized data were pre-processed and imputed resulting in a subset of 4866 genes. Differentially expressed genes were extracted with a limma *t*-test under control of multiple test, a typical issue in microarray data analysis. This analysis resulted in 528 known genes and 74 transcribed loci and unknown clones. Eighty-one percent of the total list was up-regulated and most of them are considered typical epithelial genes. In this list appeared genes or their proteins previously involved in SS (i.e., *SELL (CD62L)*, *VCAM1*, *ICAM1*, *CCL4*, *CX3CL1*, *LTF* and *IL6*) [9].

Table 1 shows the mean ratio values of the 20 top ranked genes. Ten of these 20 have been previously associated with SS [5,9,11,21–27], whereas ten (*IGHG1*, *RARRES1*, *NCF1*, *SYT1*, *HLA-DMA*, *PCOLN3*, *COL3A1*, *PRG1*, *COTL1*, *BF*) are described here for the first time associated to primary SS. This new gene set included all top ranked down-regulated genes. A complete list of all functions obtained from Gene Ontology, "Kyoto Encyclopedia of Genes and Genomes" (KEGG) and Biocarta Pathway databases is shown in Supplementary data STable 3.

Apoptotic genes represent over 10% of all known 528 differentially expressed genes. Table 2 show the relative expression of pro and anti-apoptosis genes with significative up- and down-regulation. Up-regulation of 28 pro-apoptotic genes was predominant; however 15 anti-apoptosis were also up-regulated. The genes *BCL2*, *BIRC2*, *BIRC3*, *CASP10*, *CFLAR*, *CSF2RB*, *FADD*, *IL1R1*, *NFKB1, NFKBIA*, and *TNFRSF6* belong to the KEGG's Apoptosis pathway.

Additionally, a group of 11 genes related to interferon (IFN) activity (*ICSBP1*, *MX1*, *IFITM1*, *IFIT2*, *IFI16*, *IRF7*, *NFKBIA*, *IRF9*, *IFNGR1*, *CEBPG*, *DAP*) were found over-expressed in SS samples (Table 3).

3.3. Validation of microarray results on selected genes

Our recent work has demonstrated alterations in both epithelial cells and basal lamina of LSG from SS patients [4–6]. The genes *MSN*, *VIM*, *ARPC2*, *KRT14*, *CLDN10*, *CLDN4*, *MMP9* and *VIL2* were present in the gene list and have a role in maintenance and organization of cell architecture. Accordingly, earlier reports of our group showed that MMP9 over-expression and higher levels of active MMP9 protein co-occur in severe SS patients, which yet conserve high amount of parenchyma [4,5]. In addition, MHC-class II genes have been recurrently involved in this disease [9]. Therefore, *HLA-DPA1*, *MMP-9*, *MSN* and *VIM* genes were selected to perform a side-by-side comparison of expression levels measured by microarray versus real-time PCR assays in two SS patients. As it is shown in Fig. 2A, Q-PCR and microarray results showed to be very consistent in terms of magnitude and direction. The only exception was the *MMP9* level in P3, which change in magnitude but no in direction. We also examine *MSN* levels in subjects C1, P2, P4 and P6 employing 3 dilution of template cDNA (Fig. 2B). In agreement to microarray data, *MSN* was found over-expressed in all studied

Table 1
Top ranked expressed genes in enriched LSG-epithelial cell fractions from SS patients.

Gene symbol, description	Adjusted *p*-value[a]	Gene expression (log2)	Chromosomal Location	Previously studied in SS
IGHG1, Immunoglobulin heavy constant gamma 1 (G1m marker)	0.0001	2.65	14q32.33	No
HLA-DRA, Major histocompatibility complex, class II, DR alpha	0.0005	2.20	6p21.3	Yes [9,11]
RARRES1, Retinoic acid receptor responder (tazarotene induced) 1	0.0070	2.19	3q25.32-q25.33	No
HLA-A, Major histocompatibility complex. class I A	0.0000	2.05	6p21.3	Yes [9,11,29]
NCF1, 47-kD autosomal chronic granulomatous disease protein	0.0000	1.97	7q11.23	No
SYT1, Synaptotagmin I	0.0014	1.82	12cen-q21	No
UBD, Ubiquitin	0.0007	1.74	6p21.3	Yes [11]
CXCL9, Mig Humig chemokine targeting T-cells	0.0070	1.68	4q21.1	Yes [21,22]
HLA-DRB5, Major histocompatibility complex. class II. DR beta 4	0.0016	1.54	6p21.3	Yes [27]
HLA-DRB1, Major histocompatibility complex. class II. DR beta 4	0.0004	1.49	6p21.3	Yes [9,27,31,32]
MMP9, Matrix metalloproteinase 9 gelatinase B	0.0007	1.48	20q11.2-q13.1	Yes [5]
HLA-DPA1, Major histocompatibility complex. class II. DP alpha 1	0.0004	1.47	6p21.3	Yes [11]
HLA-DMA, MHC-Class II DM alpha	0.0074	1.43	6p21.3	No
CD69, CD69 early activation antigen	0.0038	1.24	12p13-p12	Yes [26]
LTF, Lactotransferrin	0.0037	1.21	3q21-q23	Yes [23,24]
PCOLN3, Procollagen type III N-endopeptidase	0.0015	1.02	16q24.3	No
COL3A1, collagen type III alpha 1	0.0007	0.91	2q31	No
PRG1, Proteoglycan 1. secretory granule	0.0007	0.86	19q13.2	No
COTL1, Coactosin-like 1 Dictyostelium	0.0008	0.54	16q24.1	No
BF, B-factor. Properdin	0.0039	0.33	6p21.3	No

[a] The shift represents the $\log_2$ difference between the mean ratio values of all replicates of the highest (4) minus the lowest (0) focus score patient group, for the indicated gene.

samples. Finally, the MSN protein level was assayed by both immunohistochemistry and Western-blot. Green fluorescence for MSN was located at apical pole of epithelial cells (acini or ducts) in both salivary glands from SS patients or control individuals (Fig. 2C). The Western-blot pattern for MSN showed two bands at 80 and 78 kDa, these bands correspond to VIL2 and MSN respectively, which are comparable with the pattern showed by positive control (Fig. 2D). The relative levels of MSN are 1.9 higher in patients than controls. Both proteins are part from the family proteins ERM, and its identity sequence is about 78%.

3.4. Genome scan identifies potential SS susceptibility loci harboring LSG-epithelial cell expressed genes

The −log (*p*-value) of the microsatellite markers on the different human chromosomes is shown in Fig. 3. Six out of the 393 markers showed evidence of highly significant associations with primary SS in the population studied (Table 4). As expected, there was no evidence of hidden population stratification in the cohort studied. It is clear that almost 100% of the gene copies in our sample come from a single population (Supplementary data STables 4 and 5).

4. Discussion

This is the first report on the use of an enriched LSG-epithelial cell fraction in order to explore gene expression signatures from patients with primary SS and to identify SS susceptibility loci by GWAS. Therefore, our results constitute an important source of information which will help to direct future research on SS pathogenesis. Cell separation techniques from tissues containing multiple cell types are usually unable to accomplish absolute purity. The method described here produced higher yields of acini and ducts from LSG and a very low number of lymphocytic cells. Molina et al. showed in SS patients the invasion of TCD4+ and TCD8+ lymphocytes in ducts whose basal lamina were disrupted (35). This finding may explain CD 69 expression in the present study.

Apoptosis has been postulated as a mechanism for gland damage in SS and alteration of secretory function [28,30]. However, the involved mechanisms are not completely understood and, in some cases, they are contradictory. In SS patients, we found 28 pro-apoptosis and 15 anti-apoptosis related genes up-regulated (Table 2). *CASP10* up-regulation suggests that the SS-apoptotic pathway could be mediated by death receptors but modulated by the action of *CFLAR*, *MCL1* and *BIRC3* [36]. *CFLAR* encodes FLICE-inhibitory protein (FLIP), an inhibitor apoptotic protein (IAP), which inhibits caspase-10, the enzyme that is the first member of this pathway. *MCL1* belongs to the BCL2 family and down-regulates receptor-mediated apoptosis [34].*BIRC3* encodes for IAPC-2, which selectively inhibits caspases 3 and 7 and also activates their ubiquitination [36]. *CUL5* encoded a scaffold protein and a member of the E3 ubiquitin-protein ligase complex (Skp1-Cullin-F-box-typeE3 ubiquitin-protein ligase). This complex recognizes phosphorylated I-kappa-B and promotes its degradation, thus assisting in the activation of NFKB [37,38]. In this regard, PKRC phosphorylates RelA, part of the active NFKB complex, by triggering its transcriptional activity [39]. Finally, *CUL5* in combination with NFKB and IAPC-2 participates in processes that support cell survival.

The intrinsic apoptotic pathway is activated by diverse stimuli such as oxidative stress, cytokines, nitric oxide, the inflammatory infiltrate and also as a response to the anchorage loss of acinar cells from its basal lamina. The product of the *BCL2A1* gene, located in the mitochondrial membrane, is a constituent of this pathway and has a cyto-protector effect. *BNIP3L* was also up-regulated. The product of this gene forms a complex with Bcl-2, which has a pro-apoptotic effect that induces the release of cytochrome-c and proteins blocking IAPs activity (i.e. DIABLO) [40,41]. A recent study using the salivary gland-epithelial cell line A-253 showed that auto-antibodies from SS patients induce both the intrinsic and the extrinsic apoptotic pathways [42]. In human submandibular gland cells, TNF-α and IFN-γ trigger the activation of the mitochondrial death inducer, tBid, and of the intrinsic apoptotic pathway [43]. We propose that the combined action of auto-antibodies and cytokines might modulate apoptosis induction in epithelial cells from salivary glands of SS patients. To our knowledge, neither caspase-10 nor the balance of pro- and anti-apoptotic molecules participating in both apoptotic pathways has been studied in SS.

Recent reports from our laboratory have demonstrated alterations in both LSG-epithelial cells and basal lamina from SS patients [6,35,44]. The genes *MSN*, *VIM*, *ARPC2*, *KRT14*, *CLDN4*, *MMP9* and *VIL2* were present in the list of 528 genes and have a role in cell architecture, maintenance and organization [45–47]. *MSN*, *VIL2* and

Table 2
Relative expression of apoptosis-related genes in enriched LSG-epithelial cell fractions from SS patients.[a]

Gene symbol, description	Adjusted *p*-value	Gene expression (log2)	Chromosomal Location
Pro-apoptosis			
Up-regulated			
MMP9, Matrix metallopeptidase 9	0.0007	1.67	20q13.12
SRGN, Serglycin	0.0008	1.35	10q21.3
BTG1, B-cell translocation gene 1, anti-proliferative	0.0000	1.30	12q21.33
CUL3, Cullin 3	0.0008	1.23	2q36.2
PMAIP1, phorbol-12-myristate-13-acetate-induced protein 1	0.0005	1.17	18q21.32
MX1, myxovirus (influenza virus) resistance 1, interferon-inducible protein p78	0.0013	1.15	21q22.3
IFI16, interferon, gamma-inducible protein 16	0.0011	0.99	1q22
CDKN1B, cyclin-dependent kinase inhibitor 1B (p27, Kip1)	0.0000	0.90	12p13.1
TIMP3, TIMP metallopeptidase inhibitor 3	0.0086	0.90	22q12.3
ZC3H12A, Zinc finger CCCH-type containing 12A	0.0059	0.89	1p34.3
BNIP3L, BCL2/adenovirus E1B 19 kDa interacting protein 3-like	0.0055	0.83	8p21
CUL5, Cullin 5	0.0039	0.80	11q22.3
NFKBIA, nuclear factor of kappa light polypeptide gene enhancer in B-cells inhibitor, alpha	0.0109	0.80	14q13.2
EIF2AK2, eukaryotic translation initiation factor 2-alpha kinase 2	0.0011	0.75	2p22.2
GADD45G, growth arrest and DNA-damage-inducible, gamma	0.0221	0.69	9q22.2
CASP10, caspase 10, apoptosis-related cysteine peptidase	0.0253	0.65	2q33-q34
NFKB1, nuclear factor of kappa light polypeptide gene enhancer in B-cells 1 (p105)	0.0416	0.64	4q24
STK4, Serine/threonine kinase 4	0.0015	0.62	20q13.12
EP300, E1A binding protein p300	0.0058	0.52	22q13.2
CUL1, Cullin 1	0.0072	0.52	7q36.1
NAE1, NEDD8 activating enzyme E1 subunit 1	0.0258	0.48	16q22.1
FADD, Fas (TNFRSF6)-associated via death domain	0.0350	0.45	11q13.3
RRAGA, Ras-related GTP binding A	0.0273	0.44	9p22.1
PPP2CA, protein phosphatase 2 (formerly 2A), catalytic subunit, alpha isoform	0.0418	0.44	5q31.1
ATG5, autophagy related 5 homolog (S. cerevisiae)	0.0240	0.43	6q21
SMAD3, SMAD family member 3	0.0474	0.43	15q22.33
CTNNBL1, Catenin, beta like 1	0.0296	0.42	20q11.23
TIAL1, TIA1 cytotoxic granule-associated RNA binding protein-like 1	0.0343	0.40	10q
Down regulated			
PDIA3, Protein disulfide isomerase family A, member 3	0.0364	−0.54	15q15.3
PDCD4, Programmed cell death 4	0.0362	−0.61	10q25.2
DAP, death-associated protein	0.0039	−0.87	5p15.2
Anti-apoptosis			
Up-regulated			
ANXA4, Annexin A4	0.0005	1.46	2p14
IL6, interleukin 6 (interferon, beta 2)	0.0016	1.28	7p21
TNFAIP3, tumor necrosis factor, alpha-induced protein 3	0.0032	1.24	6q23.3
BIRC3, baculoviral IAP repeat-containing 3	0.0191	1.21	11q22.2
SOD2, superoxide dismutase 2, mitochondrial	0.0074	0.98	6q25.3
BCL2A1, BCL2-related protein A1	0.0100	0.80	15q25.1
ACTN3, actinin, alpha 3	0.0187	0.68	11q13.1
IGF1R, insulin-like growth factor 1 receptor	0.0246	0.62	15q26.3
SEMA4D, sema domain, immunoglobulin domain (Ig), transmembrane domain (TM) and short cytoplasmic domain, (semaphorin) 4D	0.0106	0.58	9q22.2
CDC2, Cell division cycle 2, G1 to S and G2 to M	0.0444	0.55	10q21.2
SOD1, superoxide dismutase 1, soluble	0.0063	0.52	21q22.11
TAX1BP1, Tax1 (human T-cell leukemia virus type I) binding protein 1	0.0416	0.50	7p15.2
BCL2, B-cell CLL/lymphoma 2	0.0061	0.49	18q21.3
BIRC2, baculoviral IAP repeat-containing 2	0.0410	0.47	11q22
SON, SON DNA binding protein	0.0331	0.45	21q22.11
Down regulated			
BCL2L2, BCL2-like 2	0.0311	−0.44	14q11.2
DHCR24, 24-dehydrocholesterol reductase	0.0074	−0.53	1p32.3
PHB, prohibitin	0.0124	−0.63	17q21.33
NME1, non-metastatic cells 1, protein (NM23A)	0.0014	−0.64	17q21.33
KRT18, keratin 18	0.0480	−0.65	12q13.13
PHLDA1, pleckstrin homology-like domain, family A, member 1	0.0074	−0.81	12q21.2
Dual apoptotic role			
CLU, Clusterin	0.0004	1.07	8p21.1
FAS, TNFRSF6 (TNF receptor superfamily, member 6)	0.0258	0.75	10q24.1
CFLAR, CASP8 and FADD-like apoptosis regulator	0.0403	0.65	2q33.1
BARD1, BRCA1 associated RING domain 1	0.0356	0.48	2q35

[a] A *t*-test was performed between patient and control samples with the tool Pomelo (available at http://pomelo2.bioinfo.cnio.es/). The adjusted *p*-value shown is the output of a false discovery rate (FDR) approach aimed to control multiple testing issues. The gene expression value corresponds to the difference between gene expression averages of patients minus control subjects in the $\log_2$ scale.

Table 3
Top ranked, interferon-signaling associated genes in enriched LSG-epithelial cell fractions from SS patients.

Gene symbol, description	Adjusted *p*-value	Mean Gene expression (log_2)[a]	Chromosomal Location	Previously studied in SS
ICSBP1, ICSBP Interferon consensus sequence binding protein, *IRF8*	0.017	1.47	16q24.1	Yes [11]
MX1, myxovirus (influenza virus) resistance 1, interferon-inducible protein p78	0.001	1.15	21q22.3	Yes [34]
IFITM1, interferon induced transmembrane protein 1 (9–27)	0.001	1.13	11p15.5	Yes [2,3,33]
IFIT2, Interferon-induced protein with tetratricopeptide repeats 2	0.009	1.11	10q23-q25	Yes [33]
IFI16, Interferon, gamma-inducible protein 16	0.001	0.99	1q22	Yes [4,5,33]
IRF7, Interferon regulatory factor 7	0.004	0.93	11p15.5	Yes [6,7,33]
NFKBIA, IkB alpha	0.011	0.80	14q13	Yes [8]
IRF9, interferon regulatory factor 9, *ISGF3G*	0.015	0.74	14q11.2	Yes [11]
IFNGR1, interferon gamma receptor 1, *CD119*	0.022	0.61	6q23.3	Yes [11]
CEBPG, CCAAT/enhancer binding protein (C/EBP), gamma	0.041	0.45	19q13.11	No
DAP, death associated protein	0.004	−0.87	5p15.2	No

[a] A *t*-test was performed between patient and control samples with the tool Pomelo (available at http://pomelo2.bioinfo.cnio.es/). The adjusted *p*-value shown is the output of a false discovery rate approach aimed to control multiple testing issues. The gene expression value corresponds to the difference between gene expression averages of patients minus control subjects in the log_2 scale.

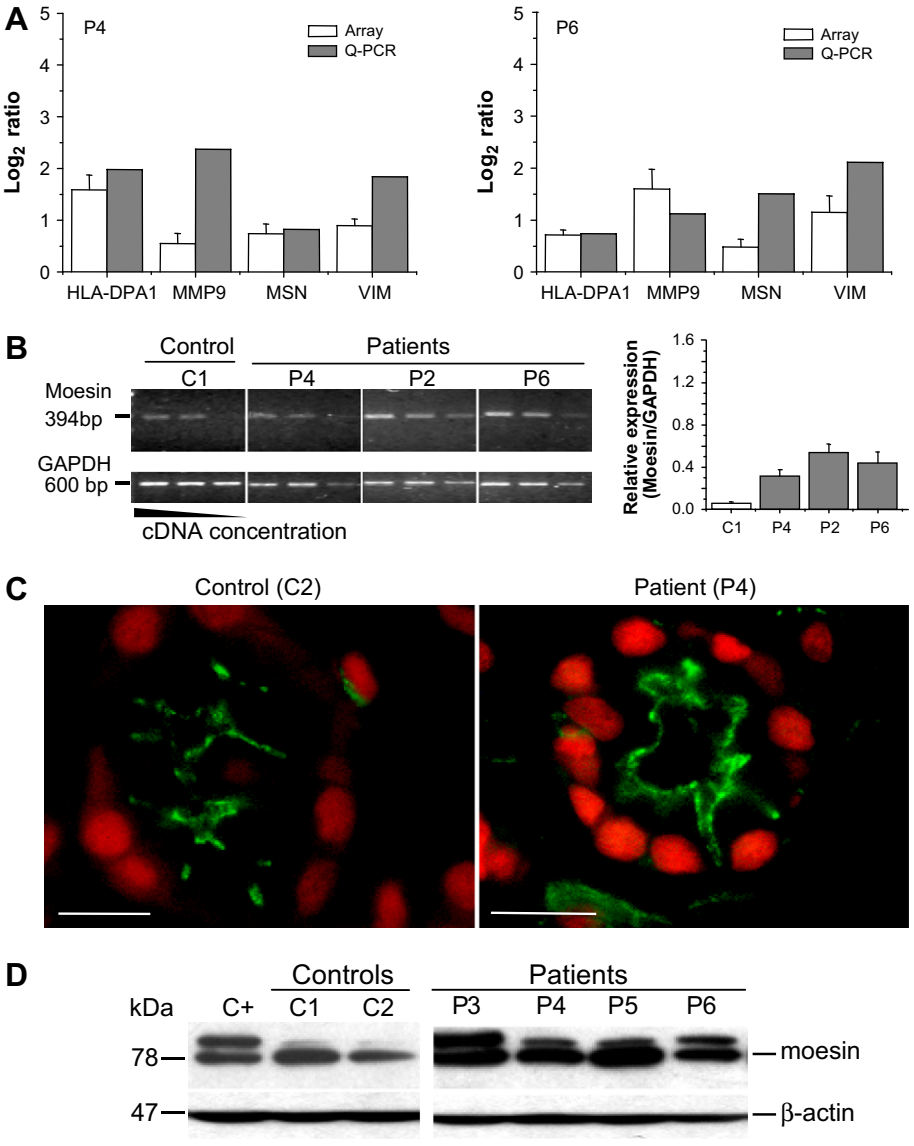

Fig. 2. Validation of the microarray results on selected genes by mRNA and protein expression. The genes *HLA-DPA1*, *MMP9*, *MSN* and *VIM* were among the statistically significant up-regulated transcripts and further validated as follows: in A), the microarray and the Q-PCR (RealTime PCR) results are contrasted for the above-mentioned genes in patients P4 and P6. In B), the RT-PCR amplification product of the moesin mRNA is shown for control (C1) and patients (P4, P2 and P6). The 3 lanes for each subject correspond to decreasing cDNA concentrations employed in the assays, as described. The reaction product of GAPDH is also shown for all assays. Bar graphic shows the densitometric analysis of semi-quantitative RT-PCR products expressed as mean MSN/GAPDH ratios of 3 independent assays. Whiskers above the bars indicate the standard error. In C), immunofluorescence images from LSG sections showing the MSN distribution in the acinar lumen for control individual (C2) and SS patient (P4). Nuclei are stained with propidium iodide (Bars = 15 μm). In D), protein levels of MSN measured by Western blot are shown for controls subjects and SS patients. The bands of 78 and 47 kD correspond to MSN and β-actin, respectively, the latter used as gel loading control.

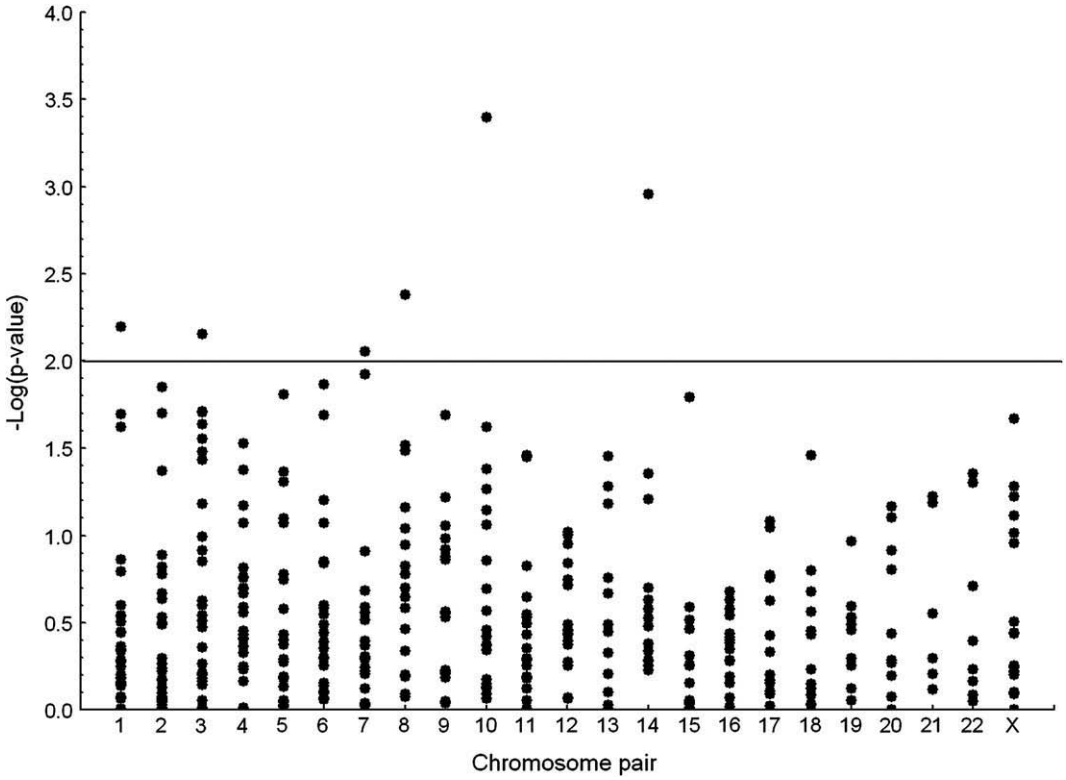

Fig. 3. Distribution of the –log(*p*-values) of the microsatellite markers on the different human chromosomes. Differences in the microsatellite allele frequencies were determined using 10,000 Markov Chain Monte Carlo simulations. We used a threshold of –log(*p*-value) = 2.0 (*p*-value = 0.01), which is indicated by the horizontal line.

CLN4 are located at the apical pole of epithelial cells. Thus their up-regulation could probably explain the disruption of this cellular compartment in SS. Real-time PCR data confirmed microarray results for *MMP9* (Fig. 2A). MMP9 over-expression has been described previously in SS LSG in relationship to the structural disorganization of acini and ducts [4].

A group of 11 genes related to IFN activity (*ICSBP1*, *MX1*, *IFITM1*, *IFIT2*, *IFI16*, *IRF7*, *NFKBIA*, *IRF9*, *IFNGR1*, *CEBPG*, *DAP*) were found up-regulated in primary SS samples (Table 3). Most of them participate in IFN signaling which suggests over-activation of this pathway [33,48]. *IFITM1* is related to the over-expression of the P48-subunit (ISGF3G) from the ISGF3 complex. In response to IFN receptor stimulation, ISGF3 (STAT2) activates the expression of genes containing the ISRE sequence (IFN sequence regulatory element) such as: *IRF7*, *G1P2*, *GBP1* and *IFITM1* [48]. IRF-7 participates in the expression of IFN-activated genes, cytokines and some chemokines [49] and it has been demonstrated that plays an essential role for a positive-loop feedback in IFN signaling [48,49]. Related studies have demonstrated that auto-antibodies (anti-SSA and/or SSB) occurring in the serum of SS patients can induce IFN expression in plasmacytoid dendritic cells (pDCs) [41,50]. LSG-ductal cells from SS patients produce high levels of CXCL9 (Mig) and CXCL10 (IP-10) chemokines while CXCL12 (SDF-1) is expressed constitutively in these glands and CXCL9 is highly expressed [22]. CXCL12 is an excellent chemoattractant for pDCs and acts in synergy with CXCL9 and CXCL10 [51]. These data could explain in part the periductal location of the focus in SS patients, in addition they suggest a close cross-talk between inhibitory and stimulatory IFN signaling to form and maintain periductal foci.

Genes related to IFN signaling have been reported in the past in SS [11,12,33,50]. This observation led to the proposal that a persistent IFN signal would induce a vicious cycle allowing a permanent activation of toll-like receptors as a response to viral RNA [12]. Recently, the activation of toll-like receptors has also been related with cleaved proteins from extracellular matrix from inflamed tissue, initiating an inflammatory response even in the absence of pathogens and infiltrating immune cells [52]. Interestingly, previous studies in our laboratory have showed an increase of these cleaved proteins in salivary glands of SS patients [6].

We used a combined approach of gene expression and GWAS to identify SS susceptibility regions harboring differentially expressed genes. From the genome-wide screen, 6 markers showed evidence of highly significant associations with SS. It is very unlikely that our results are confounded by a hidden population structure because there was no evidence of population stratification in the data. Almost 100% of the gene copies came from a single population. It is

Table 4
Microsatellite markers with significant differences in allele frequencies in SS cases and controls, and candidate's genes expressed in enriched LSG-epithelial cell fractions from SS patients.

Chromosome region	Marker	*p*-value[a]	Candidate Gen (s)[b]
1p34.2	D1S3721	0.006	*LAPTM5, ZC3H12A, NASP*
3q13.31-q13.32	D3S2460	0.007	*LTF*
7p22.2-p22.1	D7S1819	0.008	*IL6*
8q11.23	D8S1110	0.004	
10p13	D10S1430	0.0004	*CD44*
14q12	D14S608	0.001	*BCL2L2, NFKBIA, IRF9*

[a] Differences in the microsatellite allele frequencies were determined using 10,000 Markov Chain Monte Carlo simulations.

[b] As described in Santa Cruz Human Genome Project Working Draft (http://genome.ucsc.edu) and The National Center for Biotechnology Information Map Viewer (www.ncbi.nlm.nih.gov/projects/mapview) *LAPTM5:* lysosomal multi-spanning membrane protein 5, *ZC3H12A*: zinc finger CCCH-type containing 12A, *NASP:* nuclear autoantigenic sperm protein (histone-binding), *LTF*: lactotransferrin, *IL6*: interleukin-6, *BCL2L2*: BCL2-like 2, *NFKBIA*: nuclear factor of kappa light polypeptide gene enhancer in B-cells inhibitor, alpha; *IRF9:* interferon regulatory factor 9.

noteworthy that 1p34.2 (D1S3721), 3q13.31-q13.32 (D3S2460), 7p22.2-p22.1 (D7S1819), 10p13 (D10S1430), and 14q12 (D14S608) loci harbor genes differentially expressed in SS LSG-epithelial cells (Table 4), and thus worthy of further fine mapping. Besides *LAPTM5*, *LTF*, *IL6*, *CD44 and BCL2L2* genes or their respective proteins which have been previously examined in SS, *ZC3H12A*, *NASP* and *BCL2L2* are new candidate genes for the disease. ZC3H12A is an MCP1 (CCL2; MIM 158105)-induced protein that acts as a transcriptional activator [53]. *NASP* interacts with histone H1 and that this interaction occurs with high affinity, and also forms distinct, high specificity and functional complexes with histones H3 and H4 [54]. *BCL2L2*, also known as *BCL-W*, suppress apoptosis induced by over expression of either Bax or Bak [55]. Bak and its polymorphic gene have been shown to participate into the SS pathogenesis [56].

Taken together, our results show that both pro-apoptotic/anti-apoptotic and IFN signaling inhibition/stimulation balances occur in SS LSG-epithelial cells. Loci harboring the genes involved in these pathways are candidates for disease susceptibility.

Acknowledgments

We thank all the patients who participated in this study. This work was supported by Fondecyt (1080006, 1050192, and 1020755), Chile (MJG, SA, CM), MECESUP-Postgrado and Beca Conicyt (PP), Colciencias (2213-04-16715), Marshfield Foundation, and Rosario University (J-MA).

Appendix. Supplementary material

Supplementary data associated with this article can be found in the online version at doi:10.1016/j.jaut.2009.05.001

References

[1] Anaya J-M, Vega P, Correa PA, Kwon YJ, Brito M, Alliende C, et al. Síndrome de Sjögren. In: Anaya JM, Shoenfeld Y, Correa PA, García-Carrasco M, Cervera R, editors. Autoinmunidad y Enfermedad Autoinmune. Medellin: Corporación para Investigaciones Biológicas; 2005. p. 295–315.
[2] Humphreys-Beher MG, Peck AB, Dang H, Talal N. The role of apoptosis in the initiation of theautoimmune response in Sjogren's syndrome. Clin Exp Immunol 1999;116:383–7.
[3] Mitsias DI, Kapsogeorgou EK, Moutsopoulos HM. The role of epithelial cells in the initiation and perpetuation of autoimmune lesions: lessons from Sjogren's syndrome (autoimmune epithelitis). Lupus 2006;15:255–61.
[4] Perez P, Goicovich E, Alliende C, Aguilera S, Leyton C, Molina C, et al. Differential expression of matrix metalloproteinases in labial salivary glands of patients with primary Sjogren's syndrome. Arthritis Rheum 2000;43:2807–17.
[5] Perez P, Kwon YJ, Alliende C, Leyton L, Aguilera S, Molina C, et al. Increased acinar damage of salivary glands of patients with Sjogren's syndrome is paralleled by simultaneous imbalance of matrix metalloproteinase 3/tissue inhibitor of metalloproteinases 1 and matrix metalloproteinase 9/tissue inhibitor of metalloproteinases 1 ratios. Arthritis Rheum 2005;52:2751–60.
[6] Goicovich E, Molina C, Perez P, Aguilera S, Fernandez J, Olea N, et al. Enhanced degradation of proteins of the basal lamina and stroma by matrix metalloproteinases from the salivary glands of Sjogren's syndrome patients: correlation with reduced structural integrity of acini and ducts. Arthritis Rheum 2003;48:2573–84.
[7] Anaya JM, Tobon GJ, Vega P, Castiblanco J. Autoimmune disease aggregation in families with primary Sjogren's syndrome. J Rheumatol 2006;33:2227–34.
[8] Foster H, Stephenson A, Walker D, Cavanagh G, Kelly C, Griffiths I. Linkage studies of HLA and primary Sjogren's syndrome in multicase families. Arthritis Rheum 1993;36:473–84.
[9] Anaya JM, Delgado-Vega AM, Castiblanco J. Genetic basis of Sjogren's syndrome. How strong is the evidence? Clin Dev Immunol 2006;13:209–22.
[10] Killedar SJ, Eckenrode SE, McIndoe RA, She JX, Nguyen CQ, Peck AB, et al. Early pathogenic events associated with Sjogren's syndrome (SjS)-like disease of the NOD mouse using microarray analysis. Lab Invest 2006;86:1243–60.
[11] Hjelmervik TO, Petersen K, Jonassen I, Jonsson R, Bolstad AI. Gene expression profiling of minor salivary glands clearly distinguishes primary Sjogren's syndrome patients from healthy control subjects. Arthritis Rheum 2005;52:1534–44.
[12] Gottenberg JE, Cagnard N, Lucchesi C, Letourneur F, Mistou S, Lazure T, et al. Activation of IFN pathways and plasmacytoid dendritic cell recruitment in target organs of primary Sjogren's syndrome. Proc Natl Acad Sci U S A 2006;103:2770–5.
[13] Daniels TE. Labial salivary gland biopsy in Sjogren's syndrome. Assessment as a diagnostic criterion in 362 suspected cases. Arthritis Rheum 1984;27:147–56.
[14] Vitali C, Bombardieri S, Jonsson R, Moutsopoulos HM, Alexander EL, Carsons SE, et al. Classification criteria for Sjogren's syndrome: a revised version of the European criteria proposed by the American-European Consensus Group. Ann Rheum Dis 2002;61:554–8.
[15] Bravo ML, Valenzuela CY, Arcos-Burgos OM. Polymorphisms and phyletic relationships of the Paisa community from Antioquia (Colombia). Gene Geogr 1996;10:11–7.
[16] Arcos-Burgos M, Muenke M. Genetics of population isolates. Clin Genet 2002;61:233–47.
[17] Herrero J, Vaquerizas JM, Al-Shahrour F, Conde L, Mateos A, Diaz-Uriarte JS, et al. New challenges in gene expression data analysis and the extended GEPAS. Nucleic Acids Res 2004;32:W485–91.
[18] Herrero J, Al-Shahrour F, Diaz-Uriarte R, Mateos A, Vaquerizas JM, Santoyo J, et al. GEPAS: a web-based resource for microarray gene expression data analysis. Nucleic Acids Res 2003;31:3461–7.
[19] Pritchard JK, Stephens M, Donnelly P. Inference of population structure using multilocus genotype data. Genetics 2000;155:945–59.
[20] Pritchard JK, Stephens M, Rosenberg NA, Donnelly P. Association mapping in structured populations. Am J Hum Genet 2000;67:170–81.
[21] Kawasaki S, Kawamoto S, Yokoi N, Connon C, Minesaki Y, Kinoshita S, et al. Up-regulated gene expression in the conjunctival epithelium of patients with Sjogren's syndrome. Exp Eye Res 2003;77:17–26.
[22] Ogawa N, Ping L, Zhenjun L, Takada Y, Sugai S. Involvement of the interferon-gamma-induced T cell-attracting chemokines, interferon-gamma-inducible 10-kd protein (CXCL10) and monokine induced by interferon-gamma (CXCL9), in the salivary gland lesions of patients with Sjogren's syndrome. Arthritis Rheum 2002;46:2730–41.
[23] Eliasson L, Almstahl A, Lingstrom P, Wikstrom M, Carlen A. Minor gland saliva flow rate and proteins in subjects with hyposalivation due to Sjogren's syndrome and radiation therapy. Arch Oral Biol 2005;50:293–9.
[24] Haghighat N, al-Hashimi I. The status of lactoferrin and total iron binding capacity of human parotid saliva in Sjogren's syndrome. Clin Exp Rheumatol 2003;21:485–8.
[25] Hansen A, Reiter K, Ziprian T, Jacobi A, Hoffmann A, Gosemann M, et al. Dysregulation of chemokine receptor expression and function by B cells of patients with primary Sjogren's syndrome. Arthritis Rheum 2005;52:2109–19.
[26] Ohyama Y, Nakamura S, Matsuzaki G, Shinohara M, Hiroki A, Oka M, et al. T-cell receptor V alpha and V beta gene use by infiltrating T cells in labial glands of patients with Sjogren's syndrome. Oral Surg Oral Med Oral Pathol Oral Radiol Endod 1995;79:730–7.
[27] Nakken B, Jonsson R, Brokstad KA, Omholt K, Nerland AH, Haga HJ, et al. Associations of MHC class II alleles in Norwegian primary Sjogren's syndrome patients: implications for development of autoantibodies to the Ro52 autoantigen. Scand J Immunol 2001;54:428–33.
[28] Manganelli P, Fietta P. Apoptosis and Sjogren syndrome. Semin Arthritis Rheum 2003;33:49–65.
[29] Loiseau P, Lepage V, Djelal F, Busson M, Tamouza R, Raffoux C, et al. HLA class I and class II are both associated with the genetic predisposition to primary Sjogren syndrome. Hum Immunol 2001;62:725–31.
[30] Azuma T, Takei M, Yoshikawa T, Nagasugi Y, Kato M, Otsuka M, et al. Identification of candidate genes for Sjogren's syndrome using MRL/lpr mouse model of Sjogren's syndrome and cDNA microarray analysis. Immunol Lett 2002;81:171–6.
[31] Fei HM, Kang H, Scharf S, Erlich H, Peebles C, Fox R. Specific HLA-DQA and HLA-DRB1 alleles confer susceptibility to Sjogren's syndrome and autoantibody production. J Clin Lab Anal 1991;5:382–91.
[32] Kay RA, Hutchings CJ, Ollier WE. A subset of Sjogren's syndrome associates with the TCRBV13S2 locus but not the TCRBV2S1 locus. Hum Immunol 1995;42:328–30.
[33] Emamian ES, Leon JM, Lessard CJ, Grandits M, Baechler MC, Gaffney PM, et al. Peripheral blood gene expression profiling in Sjögren's syndrome. Genes Immun 2009 Apr 30 [Epub ahead of print].
[34] Wildenberg ME, van Helden-Meeuwsen CG, van de Merwe JP, Drexhage HA, Versnel MA. Systemic increase in type I interferon activity in Sjögren's syndrome: a putative role for plasmacytoid dendritic cells. Eur J Immunol 2008;38:2024–33.
[35] Molina C, Alliende C, Aguilera S, Kwon YJ, Leyton L, Martinez B, et al. Basal lamina disorganisation of the acini and ducts of labial salivary glands from patients with Sjogren's syndrome: association with mononuclear cell infiltration. Ann Rheum Dis 2006;65:178–83.
[36] Philchenkov A. Caspases: potential targets for regulating cell death. J Cell Mol Med 2004;8:432–44.
[37] Rothwarf DM, Karin M. The NF-kappa B activation pathway: a paradigm in information transfer from membrane to nucleus. Sci STKE 1999. 1999:RE1.
[38] Fay MJ, Longo KA, Karathanasis GA, Shope DM, Mandernach CJ, Leong JR, et al. Analysis of CUL-5 expression in breast epithelial cells, breast cancer cell lines, normal tissues and tumor tissues. Mol Cancer 2003;2:40.
[39] Martin AG, San-Antonio B, Fresno M. Regulation of nuclear factor kappa B transactivation. Implication of phosphatidylinositol 3-kinase and protein kinase C zeta in c-Rel activation by tumor necrosis factor alpha. J Biol Chem 2001;276:15840–9.

[40] De Laurenzi V, Melino G. Apoptosis. The little devil of death. Nature 2000;406:135–6.
[41] Strasser A. The role of BH3-only proteins in the immune system. Nat Rev Immunol 2005;5:189–200.
[42] Sisto M, Lisi S, Castellana D, Scagliusi P, D'Amore M, Caprio S, et al. Autoantibodies from Sjogren's syndrome induce activation of both the intrinsic and extrinsic apoptotic pathways in human salivary gland cell line A-253. J Autoimmun 2006;27:38–49.
[43] Lauricella M, Emanuele S, D'Anneo A, Calvaruso G, Vassallo B, Carlisi D, et al. JNK and AP-1 mediate apoptosis induced by bortezomib in HepG2 cells via FasL/caspase-8 and mitochondria-dependent pathways. Apoptosis 2006;11:607–25.
[44] Kwon YJ, Perez P, Aguilera S, Molina C, Leyton L, Alliende C, et al. Involvement of specific laminins and nidogens in the active remodeling of the basal lamina of labial salivary glands from patients with Sjogren's syndrome. Arthritis Rheum 2006;54:3465–75.
[45] Alberts B, Johnson A, Lewis J, Raff M, Roberts K, Walter E. Internal Organization of the cell. In: GS T, editor. Molecular biology of the cell. Taylor & Francis Group; 2007.
[46] Oliveira SS, Morgado-Diaz JA. Claudins: multifunctional players in epithelial tight junctions and their role in cancer. Cell Mol Life Sci 2007;64:17–28.
[47] Fievet B, Louvard D, Arpin M. ERM proteins in epithelial cell organization and functions. Biochim Biophys Acta 2007;1773:653–60.
[48] Takaoka A, Yanai H. Interferon signalling network in innate defence. Cell Microbiol 2006;8:907–22.
[49] Zhang L, Pagano JS. Structure and function of IRF-7. J Interferon Cytokine Res 2002;22:95–101.
[50] Bave U, Nordmark G, Lovgren T, Ronnelid J, Cajander S, Eloranta ML, et al. Activation of the type I interferon system in primary Sjogren's syndrome: a possible etiopathogenic mechanism. Arthritis Rheum 2005;52:1185–95.
[51] Vanbervliet B, Bendriss-Vermare N, Massacrier C, Homey B, de Bouteiller O, Briere F, et al. The inducible CXCR3 ligands control plasmacytoid dendritic cell responsiveness to the constitutive chemokine stromal cell-derived factor 1 (SDF-1)/CXCL12. J Exp Med 2003;198:823–30.
[52] Arumugam TV, Okun E, Tang SC, Thundyil J, Taylor SM, Woodruff TM. Toll-Like receptors in Ischemia-Reperfusion Injury. Shock 2008 Nov 11 [Epub ahead of print].
[53] Liang J, Wang J, Azfer A, Song W, Tromp G, Kolattukudy PE, et al. A novel CCCH-zinc finger protein family regulates proinflammatory activation of macrophages. J Biol Chem 2008;283:6337–46.
[54] Wang H, Walsh ST, Parthun MR. Expanded binding specificity of the human histone chaperone NASP. Nucleic Acids Res 2008;36:5763–72.
[55] Zhai D, Jin C, Huang Z, Satterthwait AC, Reed JC. Differential regulation of Bax and Bak by anti-apoptotic Bcl-2 family proteins Bcl-B and Mcl-1. J Biol Chem 2008;283:9580–6.
[56] Delgado-Vega AM, Castiblanco J, Gómez LM, Diaz-Gallo LM, Rojas-Villarraga A, Anaya JM. BCL2 antagonist killer 1 (BAK1) polymorphisms influence the risk of developing autoimmune rheumatic diseases in women. Ann Rheum Dis 2009 Mar 11 [Epub ahead of print].